

Single-electron transistor strongly coupled to vibrations: counting statistics and fluctuation theorem

Gernot Schaller^{1,3}, Thilo Krause¹, Tobias Brandes¹
and Massimiliano Esposito²

¹ Institut für Theoretische Physik, Technische Universität Berlin,
Hardenbergstraße 36, D-10623 Berlin, Germany

² Complex Systems and Statistical Mechanics, University of Luxembourg,
L-1511 Luxembourg, Luxembourg
E-mail: gernot.schaller@tu-berlin.de

New Journal of Physics **15** (2013) 033032 (15pp)

Received 24 October 2012

Published 22 March 2013

Online at <http://www.njp.org/>

doi:10.1088/1367-2630/15/3/033032

Abstract. Using a simple quantum master equation approach, we calculate the full counting statistics of a single-electron transistor strongly coupled to vibrations. The full counting statistics contains both the statistics of integrated particle and energy currents associated with the transferred electrons and phonons. A universal as well as an effective fluctuation theorem are derived for the general case where the various reservoir temperatures and chemical potentials are different. The first relates to the entropy production generated in the junction, while the second reveals internal information of the system. The model recovers the Franck–Condon blockade, and potential applications to non-invasive molecular spectroscopy are discussed.

³ Author to whom any correspondence should be addressed.



Content from this work may be used under the terms of the [Creative Commons Attribution-NonCommercial-ShareAlike 3.0 licence](https://creativecommons.org/licenses/by-nc-sa/3.0/). Any further distribution of this work must maintain attribution to the author(s) and the title of the work, journal citation and DOI.

Contents

1. The model	3
2. Fluctuation theorems	4
2.1. Entropy production	4
2.2. Incomplete fluctuation theorem	7
3. Counting statistics	9
4. Summary	11
Acknowledgments	11
Appendix A. Bath correlation functions for discrete phonon modes	11
Appendix B. Full counting statistics and the fluctuation theorem	13
References	15

The full counting statistics (FCS) of energy and matter exchanges provides a wealth of information about the dynamics of multi-terminal nanostructures. A great achievement of the last decade has been to conveniently identify universal features in the FCS [1–6]. Roughly speaking, these are related to the fact that fluctuations of entropy production, $\Delta_i S$, satisfy a universal fluctuation theorem (FT) $P_{+\Delta_i S}/P_{-\Delta_i S} = e^{\Delta_i S}$. At the steady state, the entropy production in the nanostructure must be balanced by the entropy flow through its terminals [7], which can be accessed through the FCS. This implies that entropy production is a measurable quantity and can be expressed as a sum of the various thermodynamic affinities acting on the system times their associated fluxes [8]. Fostered by the increased experimental abilities enabling the counting of single-electron transfers [9] and thereby the experimental verification of the FT [10], recent works have identified the non-universal FT-symmetries where an incomplete monitoring of all the terminals is performed. The resulting effective affinities may be used to probe system-specific features [11–15].

Nanoscale devices displaying coupling between electronic and vibrational transport have been widely studied in the past, in part due to their importance for thermo-electricity [16–18]. Most studies rely on the weak coupling assumption and those that do not rely on it use sophisticated self-consistent non-equilibrium Green’s function procedures. The latter often restrict the study of the FCS to the first few moments [19–22].

In this paper, we calculate the FCS for a single-electron transistor (SET) strongly coupled to a phonon bath using a new, particularly simple quantum master equation (QME) approach. We explicitly derive the universal FT in the general case where different electronic and phononic temperatures are considered. Effective FTs are also identified and both the electron and phonon average currents and Fano factors are analyzed. Going beyond heat exchange [23, 24], our model provides an efficient probe for non-destructive molecular spectroscopy: while it is known that one can determine phonon energies from electronic transport characteristics alone, the simplicity of our model allows to identify parameter regimes where this is possible without inducing further heating of phonons.

1. The model

We consider the Hamiltonian

$$H = \epsilon d^\dagger d + \sum_{k\alpha} \epsilon_{k\alpha} c_{k\alpha}^\dagger c_{k\alpha} + \sum_q \omega_q a_q^\dagger a_q + \sum_{k\alpha} \left[t_{k\alpha} d c_{k\alpha}^\dagger + \text{h.c.} \right] + d^\dagger d \sum_q \left[h_q a_q + \text{h.c.} \right] \quad (1)$$

describing a SET with two electronic leads (treated perturbatively) and additionally coupled to one or many phononic modes (treated non-perturbatively). Fermionic operators d ($c_{k\alpha}$) annihilate electrons on the dot (lead $\alpha \in \{\text{L}, \text{R}\}$) with energies ϵ ($\epsilon_{k\alpha}$), and a_q are the bosonic annihilation operators for a phonon with energy ω_q . The parameters $t_{k\alpha}$ and h_q describe electronic tunneling and phononic absorption amplitudes, respectively. For only a few phonon modes $q \in \{1, \dots, Q\}$, the model may e.g. describe electronic transport through a molecule where the electronic occupation couples to molecular vibrations. In particular, for a single phonon mode ($Q = 1$), the model represents a special case of the Anderson–Holstein model, which has previously been treated, for example, in the linear response and weak electron–phonon coupling regimes [25] or with focus on the electronic charge transfer statistics [26, 27]. For many different phonon modes or even a continuum, the model may describe more complex molecules or the interaction with bulk phonons, respectively.

Establishing the complete electronic and phononic FCS requires us to monitor not only the charge transfer but also the emitted and absorbed bosons. In principle, the statistics of the latter can be retrieved by modeling the phonons as part of the system, see e.g. [28–31]. This allows one to explore the strong electron–phonon coupling limit, but also leads to an infinitely large Hilbert space, which renders the study of the full dynamics tedious and hard to interpret. For many different phonon modes or even a continuum the required computational resources make it completely infeasible to follow this approach. Here, we therefore aim at an efficient representation with only the dot occupation treated as a dynamical variable while all electronic and phonon terminals are held at thermal equilibrium states. The challenge is to retain the complete FCS from such a reduced model. We would like to emphasize here that even in the single-phonon mode case the postulated stationarity of the phonons does not imply a weak coupling assumption between electrons and phonons. For example, for strongly coupled phonons there might exist an even faster relaxation process for the phonons immediately restoring thermal equilibrium.

After a polaron (Lang–Firsov) transformation [32, 33] $H' = e^{+S} H e^{-S}$ with $S = d^\dagger d \sum_q \left(\frac{h_q^*}{\omega_q} a_q^\dagger - \frac{h_q}{\omega_q} a_q \right)$, where

$$H' = \tilde{\epsilon} d^\dagger d + \sum_{k\alpha} \epsilon_{k\alpha} c_{k\alpha}^\dagger c_{k\alpha} + \sum_q \omega_q a_q^\dagger a_q + \sum_{k\alpha} \left[t_{k\alpha} d c_{k\alpha}^\dagger e^{-\sum_q \left(\frac{h_q^*}{\omega_q} a_q^\dagger - \frac{h_q}{\omega_q} a_q \right)} + \text{h.c.} \right] \quad (2)$$

the dot energy is renormalized $\tilde{\epsilon} \equiv \epsilon - \sum_q \frac{|h_q|^2}{\omega_q}$, and the electronic tunneling is dressed by exponentials of bosonic annihilation and creation operators. Expanding these terms demonstrates that each electronic tunneling event may now be accompanied by multiple phonon emissions and absorptions. Most important, however, we note that a perturbative treatment in the electronic tunneling amplitudes $t_{k\alpha}$ —valid for small electronic tunneling rates in comparison with the electronic reservoir temperatures—still allows for a non-perturbative treatment of the electron–phonon interaction (parameterized by h_q).

We now apply standard techniques (e.g. [2, 34]) to derive a QME containing the FCS of both the emitted/absorbed phonons and the electrons having traversed the system. Note that since we are perturbative in the electronic tunneling amplitudes, we neglect coherences and also the Kondo effect remains out of reach. For a system–bath decomposition of the form $H_{\text{SB}} = \sum_i A_i B_i$ with system and bath operators A_i and B_i , respectively, this QME requires us to calculate the bath correlation function $C_{ij}(\tau) = \langle e^{+iH_{\text{B}}\tau} B_i e^{-iH_{\text{B}}\tau} B_j \rangle$, where the expectation value is taken with respect to the stationary reservoir state [35]. In our case, the latter consists of a tensor product $\bar{\rho}_{\text{B}} = \bar{\rho}_{\text{B}}^{(\text{L})} \otimes \bar{\rho}_{\text{B}}^{(\text{R})} \otimes \bar{\rho}_{\text{B}}^{(\text{ph})}$ of different equilibrium states characterized by temperatures, and for the electronic leads also by chemical potentials. We choose the system coupling operators as $A_{1,\alpha} = d$ and $A_{2,\alpha} = d^\dagger$ and correspondingly we see that the contribution from the phonon bath enters multiplicatively in the bath coupling operators $B_{1,\alpha} = \sum_k t_{k\alpha} c_{k\alpha}^\dagger \exp[-\sum_q (\frac{h_q^*}{\omega_q} a_q^\dagger - \frac{h_q}{\omega_q} a_q)]$ and $B_{2,\alpha} = B_{1,\alpha}^\dagger$. In contrast, the contributions from the two electronic leads enter additively as usual. This leads (see appendix A for more details) to a non-standard product form of the correlation function $C_\ell(\tau) = \sum_\alpha C_\ell^{\alpha,\text{el}}(\tau) C_{\text{ph}}(\tau)$, where $\ell \in \{(12), (21)\}$. For the electronic contribution to the correlation function, we have the usual Fourier decomposition $C_\ell^{\alpha,\text{el}}(\tau) = \frac{1}{2\pi} \int \gamma_\ell^{\alpha,\text{el}}(\omega) e^{-i\omega\tau} d\omega$ with the standard electronic Fourier transforms

$$\gamma_{12}^{\alpha,\text{el}}(\omega) = \Gamma_\alpha(-\omega) f_\alpha(-\omega), \quad \gamma_{21}^{\alpha,\text{el}}(\omega) = \Gamma_\alpha(+\omega) [1 - f_\alpha(+\omega)], \quad (3)$$

where $f_\alpha(\omega) \equiv [e^{\beta_\alpha(\omega - \mu_\alpha)} + 1]^{-1}$ denotes the Fermi function of lead α held at inverse temperature β_α and chemical potential μ_α . The electronic tunneling rates in equation (3) are defined by $\Gamma_\alpha(\omega) = 2\pi \sum_k |t_{k\alpha}|^2 \delta(\omega - \epsilon_{k\alpha})$. In the following, we will parameterize them by a Lorentzian shape $\Gamma_\alpha(\omega) = \Gamma_\alpha \delta^2 / (\omega^2 + \delta^2)$ with $\delta \rightarrow \infty$ characterizing the wide-band limit. Finite δ may effectively model non-Markovian effects induced by the electronic environment [36]. Combining the phonon contributions to the bath correlation function using the Baker–Campbell–Hausdorff formula, we obtain

$$C_{\text{ph}}(\tau) = \exp \left\{ \sum_q \frac{|h_q|^2}{\omega_q^2} [e^{-i\omega_q\tau} (1 + n_{\text{B}}^q) + e^{+i\omega_q\tau} n_{\text{B}}^q - (1 + 2n_{\text{B}}^q)] \right\} \quad (4)$$

with $n_{\text{B}}^q \equiv [e^{\beta_{\text{ph}}\omega_q} - 1]^{-1}$ denoting the Bose distribution with inverse temperature β_{ph} . We note that the Fourier transform of the combined correlation function $\gamma_\ell(\omega) \equiv \int C_\ell(\tau) e^{+i\omega\tau} d\tau$ constitutes the transition rates in the rate equation when evaluated at the renormalized dot energies $\pm\tilde{\epsilon}$.

2. Fluctuation theorems

2.1. Entropy production

For a finite number of phonon modes, the FT for entropy production may be expressed in terms of the FCS, which is detailed in appendix B. This is most accessible for a single-phonon mode ($Q = 1$) at a frequency $\omega_1 = \Omega$ (we also abbreviate $n_{\text{B}}^1 \rightarrow n_{\text{B}}$ and $h_1 \rightarrow h$), where the sum in the exponential of equation (4) collapses. Then, one can identify the Fourier transform $\gamma_\ell^\alpha(\omega)$ of the correlation function via a simple integral transformation. In particular, it is straightforward to

see (see appendix A) that one can decompose $\gamma_\ell^\alpha(\omega) = \sum_{n=-\infty}^{+\infty} \gamma_{\ell,n}^\alpha(\omega)$ into processes associated with the net absorption (emission) of $n > 0$ ($n < 0$) quanta by the phonon modes

$$\gamma_{\ell,n}^\alpha(\omega) = \gamma_\ell^{\alpha,\text{el}}(\omega - n\Omega) e^{-\frac{|h|^2}{\Omega^2}(1+2n_B)} \left(\frac{1+n_B}{n_B}\right)^{n/2} \mathcal{J}_n\left(2\frac{|h|^2}{\Omega^2}\sqrt{n_B(1+n_B)}\right), \quad (5)$$

where $\mathcal{J}_n(x)$ denotes the modified Bessel function of the first kind. Firstly, in the zero-coupling limit $|h|^2 \rightarrow 0$, we recover the correlation functions of the SET (3) as all the contributions with $n \neq 0$ vanish. Secondly, in the zero-phonon-temperature limit $n_B \rightarrow 0$, only contributions for absorption by the phonon bath remain with $\lim_{n_B \rightarrow 0} [\frac{1+n_B}{n_B}]^{n/2} \mathcal{J}_n(2\frac{|h|^2}{\Omega^2}\sqrt{n_B(1+n_B)}) \stackrel{n \geq 0}{=} (\frac{|h|^2}{\Omega^2})^n \frac{1}{n!}$. Thirdly, in the wide-band ($\delta \rightarrow \infty$ such that $\Gamma_\alpha(\omega) \rightarrow \Gamma_\alpha$) and infinite bias limit ($\mu_\alpha \rightarrow \{-\infty, \infty\}$ so that $f_\alpha(\omega) \rightarrow \{0, 1\}$), we recover the standard infinite-bias results of the SET.

Both the Fermi–Dirac distribution and the Bose–Einstein distribution obey the separate relations $f_\alpha(\omega) = e^{-\beta_\alpha(\omega - \mu_\alpha)} [1 - f_\alpha(\omega)]$ and $n_B = e^{-\beta_{\text{ph}}\Omega} (1 + n_B)$. These imply that the correlation functions (5) obey a relation of the Kubo–Martin–Schwinger (KMS) type involving both electronic and phononic temperatures

$$\gamma_{12,+n}^\alpha(-\omega) = e^{-\beta_\alpha(\omega - \mu_\alpha + n\Omega)} e^{\beta_{\text{ph}}n\Omega} \gamma_{21,-n}^\alpha(+\omega) \quad (6)$$

which in the case of equal temperatures $\beta_{\text{ph}} = \beta_L = \beta_R$ reduces to the conventional KMS condition [37]. Evaluated at the renormalized dot level $\tilde{\epsilon} = \epsilon - |h|^2/\Omega$, these enter the Liouvillian \mathcal{L} of the QME describing the dot dynamics: $\dot{\rho} = \mathcal{L}\rho$, where the part acting on the populations only reads as

$$\mathcal{L} = \sum_{\alpha \in \{L,R\}} \sum_{n_\alpha = -\infty}^{+\infty} \begin{pmatrix} -\gamma_{12,n_\alpha}^\alpha & \gamma_{21,n_\alpha}^\alpha e^{+i\chi_\alpha + in_\alpha\Omega\xi_\alpha} \\ +\gamma_{12,n_\alpha}^\alpha e^{-i\chi_\alpha + in_\alpha\Omega\xi_\alpha} & -\gamma_{21,n_\alpha}^\alpha \end{pmatrix}. \quad (7)$$

Here, $\gamma_{12,n_\alpha}^\alpha \equiv \gamma_{12,n_\alpha}^\alpha(-\tilde{\epsilon})$ denotes the transition rate from an empty to a filled dot due to an electron jumping in from lead α while simultaneously triggering the absorption of n_α quanta by the phonons. Similarly, $\gamma_{21,-n_\alpha}^\alpha \equiv \gamma_{21,-n_\alpha}^\alpha(+\tilde{\epsilon})$ denotes the rate of the inverse process. Effectively, this corresponds to transport through an electronic system with infinitely many reservoirs with shifted chemical potentials, and the energetics of heat transfers is easily accessible at the level of single trajectories, see figure 1. In order to monitor the full entropy flow through the junctions, it is, in general, necessary to monitor both energy and particle flows. The electronic counting fields χ_α count the net number of electrons $n_{\text{el}}^{(\alpha)}$ jumping out of the SET to the lead α , while the phonon counting fields ξ_α count the corresponding net energy transferred to the phonons $e_{\text{ph}}^{(\alpha)} = n_\alpha\Omega$. Together, they can be used to determine the energy-particle FCS of our model, see appendix B, i.e. to calculate the time-dependent probability distribution $P_{n_{\text{el}}^{(R)}, e_{\text{ph}}^{(L)}, e_{\text{ph}}^{(R)}}(t)$ of electronic matter and the associated phonon energy transfers.

Equation (7) is a key result of our paper which clearly shows that when phonons are kept thermally equilibrated, a compact description of the dynamics can be established that keeps the full information on the electron and phonon counting statistics also in the strong electron–phonon coupling regime. In addition to thermalized phonons, the perturbative treatment of electronic tunneling requires that $\beta_\alpha\Gamma_\alpha \ll 1$. Our approach is consistent thermodynamically since as shown in appendix B, the following universal FT can be derived (also for multiple phonon modes):

$$\ln \left(\frac{P_{+n_{\text{el}}^{(R)}, +e_{\text{ph}}^{(L)}, +e_{\text{ph}}^{(R)}}(t)}{P_{-n_{\text{el}}^{(R)}, -e_{\text{ph}}^{(L)}, -e_{\text{ph}}^{(R)}}(t)} \right) \stackrel{t \rightarrow \infty}{=} A n_{\text{el}}^{(R)} + A_L e_{\text{ph}}^{(L)} + A_R e_{\text{ph}}^{(R)}, \quad (8)$$

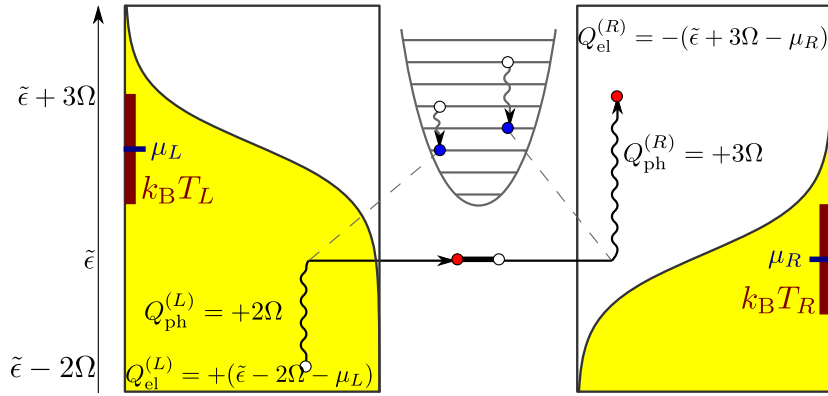


Figure 1. Sketch of the heat transfer energetics at the trajectory level for the single-phonon mode ($Q = 1$) case and for two sample elementary processes (black solid with specific heat flows into the system noted). Filled regions left and right denote Fermi functions of left and right electronic leads, whereas the sketched oscillator denotes the phonon reservoir, respectively. During the electronic tunneling events (wavy lines), energy from the phonons may assist electrons far from the dot level $\tilde{\epsilon}$ to participate in transport. In the left trajectory, an electron jumps from the left lead to the initially empty dot via the emission of two quanta by the phonons. In the right trajectory, it leaves the dot to the right lead via the emission of two quanta by the phonons. For trajectories with identical initial and final SET states (the change of SET entropy is zero), the total entropy production is minus the entropy flow and is given by $\Delta_i S = -Q_{\text{el}}^{(L)}/T_L - Q_{\text{el}}^{(R)}/T_R - (Q_{\text{ph}}^{(L)} + Q_{\text{ph}}^{(R)})/T_{\text{ph}}$, with transferred electronic heat $Q_{\text{el}}^{(\alpha)} = -(\tilde{\epsilon}n_{\text{el}}^{(\alpha)} - e_{\text{ph}}^{(\alpha)} + \mu_{\alpha}n_{\text{el}}^{(\alpha)})$ and the associated phonon heat $Q_{\text{ph}}^{(\alpha)} = -e_{\text{ph}}^{(\alpha)}$. For example, the combination of both trajectories shown yields with $n_{\text{el}}^{(L)} = -1$, $n_{\text{el}}^{(R)} = +1$, $e_{\text{ph}}^{(L)} = -2\Omega$, and $e_{\text{ph}}^{(R)} = -3\Omega$ altogether a total entropy production of $\Delta_i S = -(\tilde{\epsilon} - 2\Omega - \mu_L)/T_L - 5\Omega/T_{\text{ph}} + (\tilde{\epsilon} + 3\Omega - \mu_R)/T_R$.

where the affinities corresponding to the phonon energy and electronic fluxes are respectively, given by

$$A_{\alpha} = \beta_{\text{ph}} - \beta_{\alpha}, \quad A = (\beta_R - \beta_L)\tilde{\epsilon} + (\beta_L\mu_L - \beta_R\mu_R). \quad (9)$$

We now turn to the discussion of equation (8). Each elementary transfer process described by QME (7) involves an electron transfer between the SET and a lead α coupled to an energy transfer with the phonons. Since energy is conserved during such transfers, the energy that when $n_{\text{el}}^{(\alpha)} > 0$ leaves the SET, $\tilde{\epsilon}n_{\text{el}}^{(\alpha)}$, is equal to the energy sent to the phonons, $e_{\text{ph}}^{(\alpha)}$, plus the energy sent to lead α , $\tilde{\epsilon}n_{\text{el}}^{(\alpha)} - e_{\text{ph}}^{(\alpha)}$. As a result, the heat entering the SET from the phonons is given by $Q_{\text{ph}}^{(\alpha)} = -e_{\text{ph}}^{(\alpha)}$ and the heat entering the SET from lead α is given by $Q_{\text{el}}^{(\alpha)} = -(\tilde{\epsilon}n_{\text{el}}^{(\alpha)} - e_{\text{ph}}^{(\alpha)}) + \mu_{\alpha}n_{\text{el}}^{(\alpha)}$. For a single-phonon mode, $e_{\text{ph}}^{(\alpha)} = n_{\alpha}\Omega$, while for multiple modes, $e_{\text{ph}}^{(\alpha)} = \sum_q \omega_q n_{\alpha,q}$, where n_{α} and $n_{\alpha,q}$ denote the number of quanta with frequency Ω and ω_q that are emitted from the phonons (see appendix B for details). The entropy flow associated with this process (corresponding to minus the change in the entropy of the phonon and that of the lead α) will be given by $\Delta_e S^{(\alpha)} = \beta_{\alpha} Q_{\text{el}}^{(\alpha)} + \beta_{\text{ph}} Q_{\text{ph}}^{(\alpha)}$ [2]. At steady state, on average and in a large deviation

sense (and in a strict sense for trajectories connecting identical initial and final SET states), entropy production is equal to minus the entropy flow, i.e. $\Delta_i S = -\sum_\alpha (\beta_\alpha Q_{\text{el}}^{(\alpha)} + \beta_{\text{ph}} Q_{\text{ph}}^\alpha)$. Also, the total number of transferred electrons has to be conserved, $n_{\text{el}}^{(\text{L})} + n_{\text{el}}^{(\text{R})} = 0$. As a result, we easily verify that the entropy production $\Delta_i S$ becomes equal to equation (8).

The FT (8) thus states that trajectories with a positive entropy production occur with larger probabilities than the inverse trajectories, i.e. the expectation value of the entropy production is always positive as predicted by the second law. This holds far from equilibrium and non-perturbatively in the electron–phonon coupling strength. Single trajectories—occurring with an exponentially suppressed probability—may, however, have a negative entropy production. For example, when $\mu_{\text{L}} = \mu_{\text{R}}$, $\beta_{\text{L}} = \beta_{\text{R}} = \beta_{\text{el}}$, and $\beta_{\text{ph}} > \beta_{\text{el}}$, the combination of the two elementary processes depicted in figure 1 with $n_{\text{el}}^{(\text{R})} = +1$, $e_{\text{ph}}^{(\text{L})} = -2\Omega$ and $e_{\text{ph}}^{(\text{R})} = -3\Omega$ would yield a trajectory with negative production.

As further consistency tests of equation (8), we mention that when $\beta_{\text{el}} = \beta_{\text{R}} = \beta_{\text{L}}$, we obtain $A = \beta_{\text{el}}(\mu_{\text{L}} - \mu_{\text{R}})$ and $A_\alpha = \beta_{\text{ph}} - \beta_{\text{el}}$. When, furthermore, $\beta \equiv \beta_{\text{el}} = \beta_{\text{ph}}$, $A_\alpha = 0$ and the entropy production becomes identical to that of an isolated junction, i.e. $\Delta_i S \rightarrow \beta V_{\text{bias}} n_{\text{el}}^{(\text{R})}$ with bias voltage $V_{\text{bias}} \equiv \mu_{\text{L}} - \mu_{\text{R}}$. All affinities obviously vanish at equilibrium where $\beta_{\text{L}} = \beta_{\text{R}} = \beta_{\text{ph}}$ and $\mu_{\text{L}} = \mu_{\text{R}}$.

Finally, we mention that when phonons were treated as part of the system, the derivation of the FT would be standard due to the additivity of the electronic leads: it would not involve entropy flow across a strongly coupled terminal and thus contain no phonon-related affinity.

2.2. Incomplete fluctuation theorem

Returning to the general case but disregarding now the phonon heat counting, which is technically performed by setting $\xi_\alpha = 0$, an incomplete FT [11–15] is obtained for the probability $P_{n_{\text{el}}^{(\text{R})}}(t)$ of $n_{\text{el}}^{(\text{R})}$ electrons having crossed the junction after time t :

$$\ln \left(\frac{P_{+n_{\text{el}}^{(\text{R})}}(t)}{P_{-n_{\text{el}}^{(\text{R})}}(t)} \right) \stackrel{t \rightarrow \infty}{=} n_{\text{el}}^{(\text{R})} \cdot \sigma, \quad \sigma = \ln \left[\frac{\gamma_{12}^{\text{L}}(-\tilde{\epsilon})\gamma_{21}^{\text{R}}(+\tilde{\epsilon})}{\gamma_{12}^{\text{R}}(-\tilde{\epsilon})\gamma_{21}^{\text{L}}(+\tilde{\epsilon})} \right], \quad (10)$$

where the effective affinity σ is not universal anymore (unless $\beta_{\text{L}} = \beta_{\text{R}} = \beta_{\text{ph}}$) and can be evaluated numerically, see figure 2. Consequently, for an incomplete FT $n_{\text{el}}^{(\text{R})}\sigma$ cannot be associated anymore with the total entropy production. However, the non-universal σ does now provide additional information about the system: in the example shown in figure 2, it may, e.g., be used as an effective thermometer for the electron temperature T_{el} at a fixed phonon temperature T_{ph} . Note that flat ($\delta \rightarrow \infty$) electronic tunneling rates cancel in equation (10).

For a quantum dot coupled to *bulk* phonons (continuum of modes), obtaining the resolved FCS of different modes is realistically impossible in an experiment. Therefore, monitoring only the electronic statistics will also yield an incomplete FT. Then, the sum in equation (4) can be converted into an integral by introducing the spectral coupling density $J(\omega) = \sum_q |h_q|^2 \delta(\omega - \omega_q)$. The common choice of an Ohmic parameterization [33] $J(\omega) = J_0 \omega e^{-\omega/\omega_c}$ with the dimensionless coupling strength J_0 and cutoff frequency ω_c enables one to calculate the phonon contribution to the correlation function (4) analytically (we use an

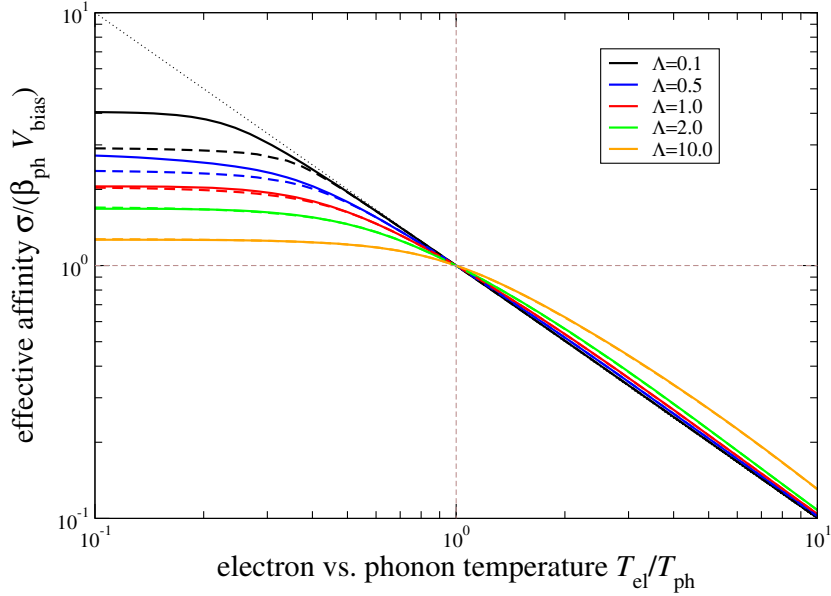


Figure 2. Effective affinity σ , equation (10), for different values of the coupling strength $\Lambda = |\hbar|^2 / \Omega^2$ in the single-mode case (solid lines) or $\Lambda = J_0$ in the continuum case (dashed curves). When $T_{\text{el}} = T_{\text{ph}}$, the FT is independent of the coupling strength (intersection point). For vanishing coupling strength, we recover $\sigma = \beta_{\text{el}}(\mu_{\text{L}} - \mu_{\text{R}})$ (dotted thin curve). Other parameters: $\Gamma_{\text{L}} = \Gamma_{\text{R}}$, $\beta_{\text{ph}}\mu_{\text{L}} = +5$, $\beta_{\text{ph}}\mu_{\text{R}} = -5$, $\delta = 10\Omega$, $\beta_{\text{ph}}\epsilon = 0$, and $\beta_{\text{ph}}\Omega = \beta_{\text{ph}}\omega_{\text{c}} = 1$.

overbar to denote the continuum case)

$$\bar{C}_{\text{ph}}(\tau) = \left[\frac{\Gamma\left(\frac{1+\beta_{\text{ph}}\omega_{\text{c}}+i\tau\omega_{\text{c}}}{\beta_{\text{ph}}\omega_{\text{c}}}\right) \Gamma\left(\frac{1+\beta_{\text{ph}}\omega_{\text{c}}-i\tau\omega_{\text{c}}}{\beta_{\text{ph}}\omega_{\text{c}}}\right)}{\Gamma^2\left(\frac{1+\beta_{\text{ph}}\omega_{\text{c}}}{\beta_{\text{ph}}\omega_{\text{c}}}\right) (1+i\tau\omega_{\text{c}})} \right]^{J_0}, \quad (11)$$

where $\Gamma(x)$ denotes the Γ -function. It is straightforward to verify a separate KMS condition in the time domain $\bar{C}_{\text{ph}}(\tau) = \bar{C}_{\text{ph}}(-\tau - i\beta_{\text{ph}})$, which implies that $\bar{\gamma}_{\text{ph}}(\omega) = e^{+\beta_{\text{ph}}\omega} \bar{\gamma}_{\text{ph}}(-\omega)$ in the frequency domain. The full Fourier transforms of the correlation functions are therefore given by a convolution integral of the separate Fourier transforms $\bar{\gamma}_{\ell}^{\alpha}(\Omega) = \frac{1}{2\pi} \int \gamma_{\ell}^{\alpha, \text{el}}(\omega) \bar{\gamma}_{\text{ph}}(\Omega - \omega) d\omega$. Using the separate electronic and phonon KMS conditions demonstrates that for equal temperatures, the conventional KMS condition must also hold in the continuum case. In addition, in the wide-band and infinite bias limits—where the electronic Fourier transforms (3) become constants (over a sufficiently wide range)—the convolution representation implies that the corresponding electronic currents are unaffected by the additional phonon reservoir. When only electrons are counted, these enter the QME as

$$\mathcal{L} = \sum_{\alpha} \begin{pmatrix} -\bar{\gamma}_{12}^{\alpha}(-\tilde{\epsilon}) & +\bar{\gamma}_{21}^{\alpha}(+\tilde{\epsilon})e^{+i\chi_{\alpha}} \\ +\bar{\gamma}_{12}^{\alpha}(-\tilde{\epsilon})e^{-i\chi_{\alpha}} & -\bar{\gamma}_{21}^{\alpha}(+\tilde{\epsilon}) \end{pmatrix}. \quad (12)$$

Again it suffices to consider only a single electronic counting field to obtain an incomplete FT as in equation (10) with $\gamma_{\ell}^{\alpha} \rightarrow \bar{\gamma}_{\ell}^{\alpha}$, where the renormalized dot level now becomes $\tilde{\epsilon} = \epsilon - J_0\omega_{\text{c}}$.

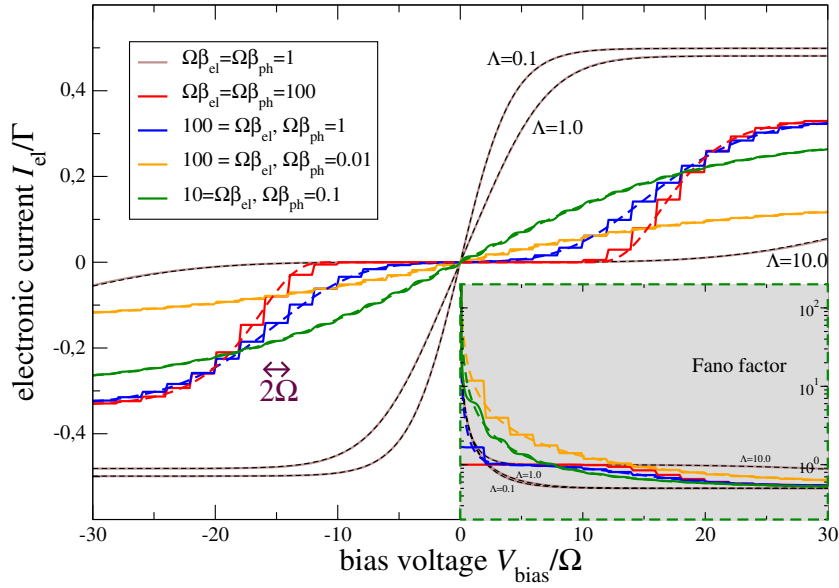


Figure 3. The electronic current and Fano factor (inset) for the single-mode (solid) and continuum (dashed) cases for different temperature configurations (colored curves) and different coupling strengths (brown solid and black dashed). Low electronic temperatures are required for resolving the single-mode nature of the phonon bath (step-like solid curves versus smooth dashed curves). The reduction of even the large-bias currents is a consequence of a constant and finite width of the electronic tunneling rates. Other parameters: $\Gamma_L = \Gamma_R = \Gamma$, $\delta = 10\Omega$, $\epsilon/\Omega = 0$, $\Omega = \omega_c$, and for the bold colored curves $\Lambda = |\hbar|^2/\Omega^2 = J_0 = 5$.

When we choose different temperatures for electrons and phonons, the affinity σ in the FT may be evaluated numerically, and displays a similar dependence as in the single-mode case provided that $J_0 = \hbar^2/\Omega^2$ and $\omega_c = \Omega$, see dashed lines in figure 2 and the discussion below.

3. Counting statistics

The cumulants of the FCS of such as electronic current $I_{el} = \frac{d}{dt} \lim_{t \rightarrow \infty} \langle n_{el}^{(R)} \rangle$ and noise $S_{el} = \frac{d}{dt} \lim_{t \rightarrow \infty} (\langle n_{el}^{(R)2} \rangle - \langle n_{el}^{(R)} \rangle^2)$ can be easily calculated using equations (7) and (12)—see, e.g., the appendix. We plot the current and Fano factor $F = S/|I|$ in figure 3. At low electronic temperatures and in the single-mode case, the phonon frequency can be deduced from the steps in the electronic current. Generally, for strong SET–phonon coupling, one observes a suppression of the finite-bias current in comparison with the uncoupled case—known as the Franck–Condon blockade [28], which normally requires us to treat phonons as dynamical degrees of freedom. Remarkably, our simple 2×2 rate equations even recover that the giant Fano factors typical of the Franck–Condon blockade can only be observed when electron and phonon temperatures are chosen as very different, i.e. when the reservoirs are unequilibrated. This behavior is found in the continuum phonon case (cf dashed curves in figure 3) as well as in

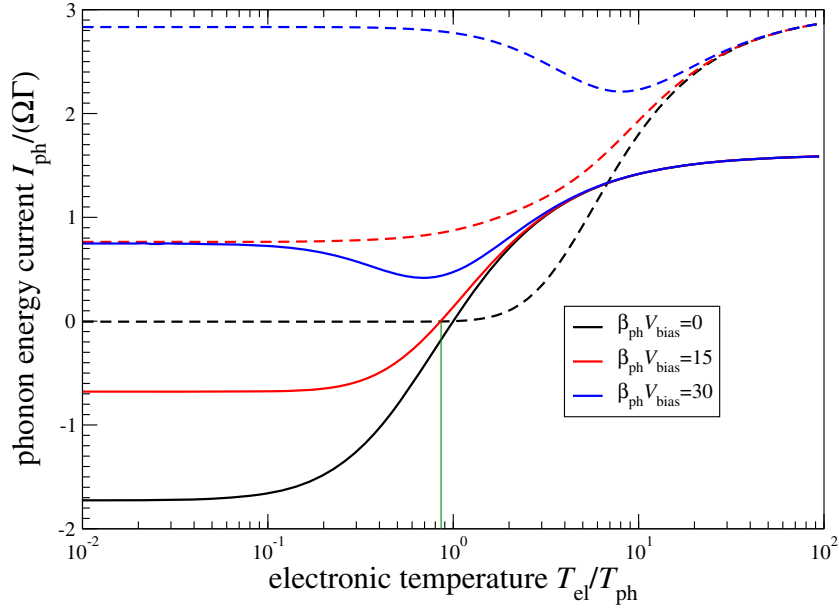


Figure 4. The total energy current into the phonon bath versus electronic temperature $T_{\text{el}}/T_{\text{ph}}$ for different phonon temperatures $\beta_{\text{ph}}\Omega = 0.1$ (solid), $\beta_{\text{ph}}\Omega = 1.0$ (dashed) and vanishing $V_{\text{bias}}\Omega = 0$ (black), intermediate $V_{\text{bias}}\Omega = 15$ (red) and high $V_{\text{bias}}\Omega = 30$ (blue) electronic bias voltages. Other parameters: $\Gamma_{\text{L}} = \Gamma_{\text{R}}$, $\delta = 10\Omega$, $\epsilon/\Omega = 0$, $\Omega\beta_{\text{ph}} = 1$, $|h|^2/\Omega^2 = 5$.

the large bias regimes ($f_{\text{L}}(\omega) \rightarrow 1$ and $f_{\text{R}}(\omega) \rightarrow 0$ but keeping the energy-dependent tunneling rates). In both wide-band and infinite bias regimes, we simply recover the conventional current of the SET (not shown).

A common problem in molecular transport spectroscopy is that the electronic current used to probe the phonon frequency will, at high bias, induce vibronic excitations, which may eventually lead to destruction of the molecule [38]. The low-dimensional model proposed here is quite useful in finding regimes allowing electronic spectroscopy (finite bias) simultaneously with a net negative phonon energy current (implying a lowering of the effective molecular temperature), see the red solid curve in figure 4. There, we evaluate the statistics of the total phonon heat emission in the single-mode case from Liouvillian (7) by not making any difference between the right and left associated electronic jumps, see the appendix. The particular parametrization in figure 4 demonstrates a stationary configuration with only slightly different electronic and phonon temperatures $T_{\text{el}} \approx 0.86 T_{\text{ph}}$ at finite bias (the intersection point of the solid red curve with $I = 0$ marked by the green vertical line), at which the phonon energy may be probed without inducing further heating. More generally, determining the phonon frequency by electronic spectroscopy in a non-destructive manner requires electron and phonon temperatures where, within a finite voltage range, the phonon heat current is non-positive. A major advantage of our model is that this range can be estimated without having to consider hundreds or thousands of phonon states.

4. Summary

We studied the combined FCS of electrons and phonons for the special case of the Anderson–Holstein model using an extremely efficient two-dimensional rate equation for the electronic populations which treats the phonon mode as a strongly coupled reservoir. Despite its simplicity, our approach was able to predict strong signatures of the Franck–Condon blockade in the electronic current and noise. Furthermore, we proved its thermodynamic consistency by explicitly deriving a universal FT for the entropy production and identifying the three thermodynamic affinities characterizing our setup and imposing universal symmetries on the FCS. Our results hold for arbitrary electron–phonon coupling and also for multiple phonon modes as long as they are held at thermal equilibrium. In addition, we found a non-universal FT referring only to the electronic counting statistics, which may be used to probe the phonon temperature. The universal FT is recovered in this case when all terminal temperatures are set equal, which implies that the energy flow between the system and the phonons vanishes. Due to its small dimensionality, our model may prove useful in identifying appropriate regimes for performing non-destructive molecular spectroscopy. Furthermore, we expect our approach to be applicable also to electronic transport through more complex structures.

Acknowledgments

Financial support from the DFG (SCHA 1646/2-1, SFB 910 and GRK 1558) and the National Research Fund, Luxembourg (project no. FNR/A11/02) is gratefully acknowledged. The authors have profited from discussions with G Kiesslich and P Strasberg.

Appendix A. Bath correlation functions for discrete phonon modes

Obviously, the phonon correlation function equation (4) can be written as a product of single-mode correlation functions

$$C_{\text{ph}}(\tau) = \prod_{q=1}^Q C_{\text{ph}}^q(\tau), \quad (\text{A.1})$$

where Q denotes the number of different phonon modes. Each factor can be formally expanded in the variables $e^{\pm i\omega_q \tau}$

$$\begin{aligned} C_{\text{ph}}^q(\tau) &= e^{-\frac{|h_q|^2}{\omega_q^2}(1+2n_B^q)} \sum_{m,m'=0}^{\infty} \left(\frac{|h_q|^2}{\omega_q^2} \right)^{m+m'} \frac{(n_B^q)^m (1+n_B^q)^{m'}}{m!m'} e^{+i(m-m')\omega_q \tau} \\ &\equiv \sum_{m,m'=0}^{\infty} C_{mm',\text{ph}}^q(\tau). \end{aligned} \quad (\text{A.2})$$

Now, the key observation is that the terms in the sum can be interpreted as accounting for the emission (absorption) by the phonons of m (m') quanta with frequency ω_q . Since we are interested in the net number of quanta absorption by the phonon bath $n = m' - m$, it is natural to define

$$C_{n,\text{ph}}^q(\tau) \equiv \sum_{m,m'}^{\infty} \delta(m' - m, n) C_{mm',\text{ph}}^q(\tau) \quad (\text{A.3})$$

with $\delta(m, m')$ denoting the Kronecker symbol. The identity

$$\begin{aligned}
 f(a, b, n) &= \sum_{m, m'=0}^{\infty} \frac{a^m b^{m'}}{m! m'!} \delta(m' - m, n) \\
 &= \begin{cases} \sum_{m=0}^{\infty} \frac{a^m b^{m+n}}{m! (m+n)!}, & n \geq 0 \\ \sum_{m=-n}^{\infty} \frac{a^m b^{m+n}}{m! (m+n)!}, & n < 0 \end{cases} \\
 &= \left(\frac{b}{a}\right)^{n/2} \mathcal{J}_n(2\sqrt{ab}),
 \end{aligned} \tag{A.4}$$

where $\mathcal{J}_n(x)$ denotes the modified Bessel function of the first kind, takes the summation boundaries into account properly and implies that

$$\begin{aligned}
 C_{\text{ph}}^q(\tau) &= \sum_{n=-\infty}^{+\infty} C_{n, \text{ph}}^q(\tau) \\
 &= \sum_{n=-\infty}^{+\infty} e^{-in\omega_q \tau} e^{-\frac{|h_q|^2}{\omega_q^2} (1+2n_B^q)} \left(\frac{1+n_B^q}{n_B^q}\right)^{\frac{n}{2}} \mathcal{J}_n\left(2\frac{|h_q|^2}{\omega_q^2} \sqrt{n_B^q (1+n_B^q)}\right).
 \end{aligned} \tag{A.5}$$

For the full phonon correlation function, we can separate the τ -dependence as

$$\begin{aligned}
 C_{\text{ph}}(\tau) &= \sum_{\mathbf{n}} e^{-i\mathbf{n} \cdot \boldsymbol{\Omega} \tau} \prod_{q=1}^Q \left[e^{-\frac{|h_q|^2}{\omega_q^2} (1+2n_B^q)} \left(\frac{1+n_B^q}{n_B^q}\right)^{\frac{n_q}{2}} \mathcal{J}_{n_q}\left(2\frac{|h_q|^2}{\omega_q^2} \sqrt{n_B^q (1+n_B^q)}\right) \right] \\
 &\equiv \sum_{\mathbf{n}} e^{-i\mathbf{n} \cdot \boldsymbol{\Omega} \tau} C_{\text{ph}}^{\mathbf{n}},
 \end{aligned} \tag{A.6}$$

where $\sum_{\mathbf{n}} \equiv \sum_{n_1=-\infty}^{+\infty}, \dots, \sum_{n_Q=-\infty}^{+\infty}$ such that each phonon mode has a different summation index and $\mathbf{n} \equiv (n_1, \dots, n_Q)$, $\boldsymbol{\Omega} \equiv (\omega_1, \dots, \omega_Q)$ with $\mathbf{n} \cdot \boldsymbol{\Omega} = \sum_{q=1}^Q n_q \omega_q$. This enables one to express the Fourier transform of the total (electron and phonon) bath correlation function

$$\begin{aligned}
 \gamma_{\ell}^{\alpha}(\omega) &= \int d\tau C_{\ell}^{\alpha, \text{el}}(\tau) C_{\text{ph}}(\tau) e^{+i\omega \tau} \\
 &= \sum_{\mathbf{n}_{\alpha}} \int d\tau \left[\frac{1}{2\pi} \int d\omega' \gamma_{\ell}^{\alpha, \text{el}}(\omega') e^{-i\omega' \tau} \right] e^{+i(\omega - \mathbf{n}_{\alpha} \cdot \boldsymbol{\Omega}) \tau} C_{\text{ph}}^{\mathbf{n}_{\alpha}} \\
 &= \sum_{\mathbf{n}_{\alpha}} \gamma_{\ell}^{\alpha, \text{el}}(\omega - \mathbf{n}_{\alpha} \cdot \boldsymbol{\Omega}) C_{\text{ph}}^{\mathbf{n}_{\alpha}} \equiv \sum_{\mathbf{n}_{\alpha}} \gamma_{\ell, \mathbf{n}_{\alpha}}^{\alpha}(\omega)
 \end{aligned} \tag{A.7}$$

as a weighted superposition of purely electronic Fourier transforms that are evaluated at phonon-shifted frequencies. Each term $\gamma_{\ell, \mathbf{n}_{\alpha}}^{\alpha}$ in the sum accounts for a single electronic jump across junction α triggering the net absorption by the phonons of $(n_{\alpha, 1}, \dots, n_{\alpha, Q})$ quanta carrying a net energy of $e_{\alpha} = \mathbf{n}_{\alpha} \cdot \boldsymbol{\Omega}$. In particular, for a single-phonon mode ($Q = 1$), this leads to equation (5) of this paper.

The discussion in the paper, however, applies also to multiple phonon modes at the same temperature: the bosonic symmetry relation $n_B^q = e^{-\beta_{\text{ph}}\omega_q} (1 + n_B^q)$, for example, implies for the weight factors in equation (A.6)

$$C_{\text{ph}}^{-n_\alpha} = e^{-\beta_{\text{ph}}n_\alpha \cdot \Omega} C_{\text{ph}}^{+n_\alpha} \quad (\text{A.8})$$

which can be used to show that the single-mode KMS relation (6) in the paper straightforwardly generalizes to

$$\gamma_{12,+n_\alpha}^\alpha(-\omega) = e^{-\beta_\alpha(\omega - \mu_\alpha + n_\alpha \cdot \Omega)} e^{\beta_{\text{ph}}n_\alpha \cdot \Omega} \gamma_{21,-n_\alpha}^\alpha(+\omega), \quad (\text{A.9})$$

where $e_\alpha = n_\alpha \cdot \Omega$ is the total net energy absorbed by the phonon bath when an electronic transition with lead α occurs. For the total entropy production, this total transferred energy e_α is relevant. Therefore, when inserting counting fields into the Liouvillian, it suffices to count the net bosonic energy transfer triggered by electronic jumps across each junction instead of counting each phonon mode separately, such that equation (7) in the paper generalizes to

$$\mathcal{L}(\chi, \xi_L, \xi_R) = \sum_{\alpha \in \{L,R\}} \sum_{n_\alpha} \begin{pmatrix} -\gamma_{12,n_\alpha}^\alpha(-\tilde{\epsilon}) & \gamma_{21,n_\alpha}^\alpha(+\tilde{\epsilon}) e^{+i\chi_\alpha} e^{+ie_\alpha \xi_\alpha} \\ +\gamma_{12,n_\alpha}^\alpha(-\tilde{\epsilon}) e^{-i\chi_\alpha} e^{+ie_\alpha \xi_\alpha} & -\gamma_{21,n_\alpha}^\alpha(+\tilde{\epsilon}) \end{pmatrix} \quad (\text{A.10})$$

with the renormalized dot level $\tilde{\epsilon} = \epsilon - \sum_{q=1}^Q \frac{|h_q|^2}{\omega_q}$. The dimensionless electronic counting fields χ_α enable one to extract the complete electronic particle counting statistics. In contrast, the phonon energy counting fields ξ_α have dimension of inverse energy and account for the statistics of phonon-related energy transfers triggered by electronic jumps across junction α . For the case of a single-phonon mode (see the main paper), the total phonon energy and phonon number for electronic jumps across junction α are tightly coupled, $e_\alpha = n_\alpha \Omega$, such that the full energy counting statistics for the phonons also yields the full particle counting statistics. To obtain the full particle counting statistics for multi-mode phonons one would have to make the counting fields mode-dependent $e^{in_\alpha \cdot \Omega \xi_\alpha} \rightarrow e^{i \sum_{q=1}^Q n_{\alpha,q} \xi_{\alpha,q}}$, which would exceed the focus of this paper.

Appendix B. Full counting statistics and the fluctuation theorem

The counting-field-dependent Liouvillian (A.10) and its single-mode version (7) enable the construction of the FCS, i.e. the probability $P_{n_{\text{el}}^{(L)}, n_{\text{el}}^{(R)}, e_{\text{ph}}^{(L)}, e_{\text{ph}}^{(R)}}(t)$ to observe $n_{\text{el}}^{(\alpha)}$ net electrons transfers to lead α and a net associated energy $e_{\text{ph}}^{(\alpha)}$ absorbed by the phonon reservoir. We are interested in the large-time limit, due to charge conservation, it suffices to consider a single electronic counting field. In the following, we will therefore consider $\chi_L = 0$ and $\chi_R = \chi$ leading to the probability distribution $P_{n_{\text{el}}^{(R)}, e_{\text{ph}}^{(L)}, e_{\text{ph}}^{(R)}}(t)$ associated with $n_{\text{el}}^{(R)}$ net electrons emitted into the right reservoir. It is technically convenient to construct cumulants of the probability distribution via the cumulant-generating function (CGF), which in the long-term limit becomes

$$\mathcal{C}(\chi, \xi_L, \xi_R, t) \xrightarrow{t \rightarrow \infty} \lambda(\chi, \xi_L, \xi_R) t, \quad (\text{B.1})$$

where $\lambda(\chi, \xi_L, \xi_R)$ denotes the dominant eigenvalue of the Liouvillian which vanishes when all counting fields are set to zero, $\lambda(0, 0, 0) = 0$. Cumulants are obtained by taking derivatives with respect to the counting field of interest: the trivial long-term time dependence then enables one to consider the CGF for the currents $\lambda(\chi, \xi_L, \xi_R)$ instead, such that the electronic particle current and noise at the right junction, for example, may be obtained via

$$I = (-i) \partial_\chi \lambda(\chi, 0, 0)|_{\chi=0}, \quad S = (-i)^2 \partial_\chi^2 \lambda(\chi, 0, 0)|_{\chi=0}. \quad (\text{B.2})$$

Similarly, the total phonon energy current and noise follow by disregarding the difference between left- and right-associated emissions

$$I_{\text{ph}} = (-i)\partial_{\xi} \lambda(0, \xi, \xi)|_{\xi=0}, \quad S_{\text{ph}} = (-i)^2\partial_{\xi}^2 \lambda(0, \xi, \xi)|_{\xi=0}. \quad (\text{B.3})$$

The full distribution may be obtained from the CGF by performing an inverse Fourier transform, which in the long-term limit becomes

$$P_{n_{\text{el}}^{(\text{R})}, e_{\text{ph}}^{(\text{L})}, e_{\text{ph}}^{(\text{R})}}(t) \xrightarrow{t \rightarrow \infty} \int_{-\pi}^{+\pi} \frac{d\chi}{2\pi} \int_{-\infty}^{+\infty} \frac{d\xi_{\text{L}}}{2\pi} \int_{-\infty}^{+\infty} \frac{d\xi_{\text{R}}}{2\pi} e^{\lambda(\chi, \xi_{\text{L}}, \xi_{\text{R}})t} e^{-i(n_{\text{el}}^{(\text{R})}\chi + e_{\text{ph}}^{(\text{L})}\xi_{\text{L}} + e_{\text{ph}}^{(\text{R})}\xi_{\text{R}})}. \quad (\text{B.4})$$

From the properties of the Fourier transform, it follows that a shift symmetry of the CGF is associated with an FT for the FCS, i.e.

$$\lambda(-\chi, -\xi_{\text{L}}, -\xi_{\text{R}}) = \lambda(+\chi + iA, +\xi_{\text{L}} + iA_{\text{L}}, +\xi_{\text{R}} + iA_{\text{R}})$$

$$\iff$$

$$\lim_{t \rightarrow \infty} \ln \frac{P_{+n_{\text{el}}^{(\text{R})}, +e_{\text{ph}}^{(\text{L})}, +e_{\text{ph}}^{(\text{R})}}(t)}{P_{-n_{\text{el}}^{(\text{R})}, -e_{\text{ph}}^{(\text{L})}, -e_{\text{ph}}^{(\text{R})}}(t)} = n_{\text{el}}^{(\text{R})}A + e_{\text{ph}}^{(\text{L})}A_{\text{L}} + e_{\text{ph}}^{(\text{R})}A_{\text{R}}. \quad (\text{B.5})$$

We aim at obtaining the affinities A , A_{L} , and A_{R} , which with equation (B.1) yield a long-term symmetry of the CGF. In our model (A.10), it is most convenient to derive the corresponding symmetry from the characteristic polynomial of the Liouvillian.

To see it, we first write the off-diagonal matrix elements of the Liouvillian as explicit functions of the counting fields (the diagonal entries do not depend on the counting fields)

$$\begin{aligned} \mathcal{L}_{12}(+\chi, +\xi_{\text{L}}, +\xi_{\text{R}}) &= \sum_n (\gamma_{21,n}^{\text{L}}(+\tilde{\epsilon})e^{+in\Omega\xi_{\text{L}}} + \gamma_{21,n}^{\text{R}}(+\tilde{\epsilon})e^{+i\chi} e^{+in\Omega\xi_{\text{R}}}), \\ \mathcal{L}_{21}(+\chi, +\xi_{\text{L}}, +\xi_{\text{R}}) &= \sum_n (\gamma_{12,n}^{\text{L}}(-\tilde{\epsilon})e^{+in\Omega\xi_{\text{L}}} + \gamma_{12,n}^{\text{R}}(-\tilde{\epsilon})e^{-i\chi} e^{+in\Omega\xi_{\text{R}}}), \end{aligned} \quad (\text{B.6})$$

where we recall that $\chi_{\text{L}} = 0$ and $\chi_{\text{R}} = \chi$. Inserting the KMS condition (A.9) and replacing $n \rightarrow -n$ under the sum, we obtain

$$\begin{aligned} \mathcal{L}_{12}(-\chi, -\xi_{\text{L}}, -\xi_{\text{R}}) &= \sum_n \left(\gamma_{12,n}^{\text{L}}(-\tilde{\epsilon})e^{+in\Omega\xi_{\text{L}}} e^{-(\beta_{\text{ph}} - \beta_{\text{L}})n\Omega} e^{\beta_{\text{L}}(\tilde{\epsilon} - \mu_{\text{L}})} \right. \\ &\quad \left. + \gamma_{12,n}^{\text{R}}(-\tilde{\epsilon})e^{-i\chi} e^{+in\Omega\xi_{\text{R}}} e^{-(\beta_{\text{ph}} - \beta_{\text{R}})n\Omega} e^{\beta_{\text{R}}(\tilde{\epsilon} - \mu_{\text{R}})} \right) \\ &= e^{+\beta_{\text{L}}(\tilde{\epsilon} - \mu_{\text{L}})} \mathcal{L}_{21}(\chi + iA, \xi_{\text{L}} + iA_{\text{L}}, \xi_{\text{R}} + iA_{\text{R}}) \end{aligned} \quad (\text{B.7})$$

with $A = \beta_{\text{R}}(\tilde{\epsilon} - \mu_{\text{R}}) - \beta_{\text{L}}(\tilde{\epsilon} - \mu_{\text{L}})$, $A_{\text{L}} = \beta_{\text{ph}} - \beta_{\text{L}}$ and $A_{\text{R}} = \beta_{\text{ph}} - \beta_{\text{R}}$. This symmetry is equivalent to

$$\mathcal{L}_{21}(-\chi, -\xi_{\text{L}}, -\xi_{\text{R}}) = e^{-\beta_{\text{L}}(\tilde{\epsilon} - \mu_{\text{L}})} \mathcal{L}_{12}(\chi + iA, \xi_{\text{L}} + iA_{\text{L}}, \xi_{\text{R}} + iA_{\text{R}}). \quad (\text{B.8})$$

The characteristic polynomial can be written as

$$\begin{aligned} \mathcal{D}(\chi, \xi_{\text{L}}, \xi_{\text{R}}) &= |\mathcal{L}(\chi, \xi_{\text{L}}, \xi_{\text{R}}) - \lambda \mathbf{1}| \\ &= (\mathcal{L}_{11} - \lambda)(\mathcal{L}_{22} - \lambda) - \mathcal{L}_{21}(\chi, \xi_{\text{L}}, \xi_{\text{R}})\mathcal{L}_{12}(\chi, \xi_{\text{L}}, \xi_{\text{R}}), \end{aligned} \quad (\text{B.9})$$

where we see that when evaluating the expression at negative arguments the exponential prefactors from equations (B.7) and (B.8) cancel and we easily read off the symmetry

$$\mathcal{D}(-\chi, -\xi_{\text{L}}, -\xi_{\text{R}}) = \mathcal{D}(+\chi + iA, +\xi_{\text{L}} + iA_{\text{L}}, +\xi_{\text{R}} + iA_{\text{R}}). \quad (\text{B.10})$$

Since the two eigenvalues of the Liouvillian $\lambda(\chi, \xi_L, \xi_R)$ and $\bar{\lambda}(\chi, \xi_L, \xi_R)$ are given by the roots of the characteristic polynomial $\mathcal{D}(\chi, \xi_L, \xi_R) = [\lambda - \lambda(\chi, \xi_L, \xi_R)][\lambda - \bar{\lambda}(\chi, \xi_L, \xi_R)]$, this symmetry transfers to the long-term CGF as

$$\lambda(-\chi, -\xi_L, -\xi_R) = \lambda(+\chi + iA, +\xi_L + iA_L, +\xi_R + iA_R) \quad (\text{B.11})$$

and eventually implies the validity of the full FT (8) in the main text.

References

- [1] Tobiska J and Nazarov Y V 2005 *Phys. Rev. B* **72** 235328
- [2] Esposito M, Harbola U and Mukamel S 2009 *Rev. Mod. Phys.* **81** 1665
- [3] Andrieux D, Gaspard P, Monnai T and Tasaki S 2009 *New J. Phys.* **11** 043014
- [4] Utsumi Y and Saito K 2009 *Phys. Rev. B* **79** 235311
- [5] Campisi M, Hänggi P and Talkner P 2011 *Rev. Mod. Phys.* **83** 771
- [6] Utsumi Y, Entin-Wohlman O, Ueda A and Aharony A 2013 *Phys. Rev. B* **87** 115407
- [7] Lebowitz J L and Spohn H 1999 *J. Stat. Phys.* **95** 333
- [8] Andrieux D and Gaspard P 2007 *J. Stat. Phys.* **127** 107
- [9] Fujisawa T, Hayashi T, Tomita R and Hirayama Y 2006 *Science* **312** 1634
- [10] Utsumi Y, Golubev D S, Marthaler M, Saito K, Fujisawa T and Schön G 2010 *Phys. Rev. B* **81** 125331
- [11] Sánchez R, Lopez R, Sanchez D and Büttiker M 2010 *Phys. Rev. Lett.* **104** 076801
- [12] Krause T, Schaller G and Brandes T 2011 *Phys. Rev. B* **84** 195113
- [13] Bulnes Cuetara G, Esposito M and Gaspard P 2011 *Phys. Rev. B* **84** 165114
- [14] Ganeshan S and Sinityn N A 2011 *Phys. Rev. B* **84** 245405
- [15] Golubev D S, Utsumi Y, Marthaler M and Schön G 2011 *Phys. Rev. B* **84** 075323
- [16] Segal D 2005 *Phys. Rev. B* **72** 165426
- [17] Esposito M, Lindenberg K and Van den Broeck C 2009 *Europhys. Lett.* **85** 60010
- [18] Dubi Y and Di Ventra M 2011 *Rev. Mod. Phys.* **83** 131
- [19] Galperin M, Nitzan A and Ratner M A 2006 *Phys. Rev. B* **73** 045314
- [20] Galperin M, Nitzan A and Ratner M A 2008 *Mol. Phys.* **106** 397
- [21] Haupt F, Novotny T and Belzig W 2009 *Phys. Rev. Lett.* **103** 136601
- [22] Park T-H and Galperin M 2011 *Phys. Rev. B* **84** 205450
- [23] Nicolin L and Segal D 2011 *Phys. Rev. B* **84** 161414
- [24] Nicolin L and Segal D 2011 *J. Chem. Phys.* **135** 164106
- [25] Entin-Wohlman O, Imry Y and Aharony A 2010 *Phys. Rev. B* **82** 115314
- [26] Maier S, Schmidt T L and Komnik A 2011 *Phys. Rev. B* **83** 085401
- [27] White A J and Galperin M 2012 *Phys. Chem. Phys.* **14** 13809
- [28] Koch J and von Oppen F 2005 *Phys. Rev. Lett.* **94** 206804
- [29] Segal D 2008 *Phys. Rev. Lett.* **100** 105901
- [30] Avriller R 2011 *J. Phys.: Condens. Matter* **23** 105301
- [31] Mitra A, Aleiner I and Millis A J 2004 *Phys. Rev. B* **69** 245302
- [32] Mahan G D 1990 *Many-Particle Physics* (New York: Plenum)
- [33] Brandes T 2005 *Phys. Rep.* **408** 315
- [34] Schaller G, Kießlich G and Brandes T 2009 *Phys. Rev. B* **80** 245107
- [35] Breuer H-P and Petruccione F 2002 *The Theory of Open Quantum Systems* (Oxford: Oxford University Press)
- [36] Zedler P, Schaller G, Kießlich G, Emary C and Brandes T 2009 *Phys. Rev. B* **80** 045309
- [37] Weiss U 1993 *Quantum Dissipative Systems Modern Condensed Matter Physics 2* (Singapore: World Scientific)
- [38] Simine L and Segal D 2012 *Phys. Chem. Chem. Phys.* **14** 13820